Electronic resonant images of an ion implanted Si(111) substrate observed by wavelength tunable optical second harmonic microscopy

Haruyuki Sano,[a] Jun Saito, Junichi Ikeda, and Goro Mizutani
School of Materials Science, Japan Advanced Institute of Science and Technology, 1-1 Asahidai, Nomi, Ishikawa 923-1292, Japan

(Received 22 February 2006; accepted 1 June 2006; published online 23 August 2006)

This paper demonstrates that the spatial distribution of electronic states of an arsenic ion implanted Si(111) substrate can be observed by using a wavelength tunable second harmonic (SH) microscope in a wide photon energy range from $2\hbar\omega=1.96$ to 5.19 eV. The contrast in the SH intensity images between the As-doped area and the nondoped area depends greatly on the SH photon energy. For $2\hbar\omega>3$ eV, optical second harmonic generation (SHG) from the nondoped area was stronger than from the doped area, and the contrast was reversed for $2\hbar\omega\leqslant 2.33$ eV. The contrast in the SH intensity images was considerably different from that in the linear optical reflection images, indicating that spectroscopic SH microscopy can provide different informations on electronic levels from that associated with the linear optical response. It is suggested that the larger SH intensity from the nondoped area for $2\hbar\omega>3$ eV results from the resonant SHG enhancement effect associated with the bulk Si E_1 (3.4 eV) and E_2 (4.3 eV) gaps. In the case of the doped area, a small resonant enhancement of the SH intensity was observed around $2\hbar\omega=2.33$ eV. This resonance may result from an energy level created by the ion implantation. © *2006 American Institute of Physics*.
[DOI: 10.1063/1.2266158]

I. INTRODUCTION

Optical second harmonic generation (SHG) is the lowest-order nonlinear optical process that occurs in media without inversion symmetry. Since the SH response is highly sensitive to the symmetry of the atomic structure and electronic states, SHG has been used as a powerful probe in various research fields, e.g., surface science,[1–3] magnetism,[4] and biochemistry.[5] Recently, SHG has been applied to the microscopy of magnetic materials,[6,7] ferroelectric materials,[8–10] metals,[11,12] semiconductors,[13–15] and biomaterials.[16–19] In most of these experiments only a limited number of wavelengths, such as 1064 and 532 nm from a Nd:YAG (yttrium aluminium garnet) laser and ~800 nm from a Ti:sapphire laser, have been used for excitation.

When the incident or SH photon energy is close to the electronic transition energies in a material, the SH light intensity is remarkably enhanced due to the resonance effect.[20] Therefore, the spatial distribution of particular electronic states should be obtained from the SH intensity images by the excitation light of resonant wavelengths from a tunable laser. This experimental method, i.e., spectroscopic SH microscopy, is expected to be a useful method for analyzing the electronic states of materials. However, only a few studies using it have been reported so far.[6,15,21] In these experimental studies, noncentrosymmetric compound semiconductor crystals such as InAlGaAs (Ref. 15) and ZnSe (Ref. 21) were adopted as samples. Since noncentrosymmetric materials emit intense SH light, it should be relatively easy to obtain SH images from them. On the other hand, an elementary semiconductor with a centrosymmetric structure such as Si is difficult to observe by spectroscopic SH microscopy and has not been investigated, though it is one of the most important materials in both basic and applied physics.

The goal of our study is to establish spectroscopic SH microscopy as a powerful probe capable of obtaining unique findings about the electronic states of various materials. For this goal, the following two demonstrations are required: that a weak SH signal from a material with inversion symmetry is observable, and that spectroscopic SH microscopy can provide electronic resonant images different from those obtained by conventional linear optical microscopy. Achieving these demonstrations is the main purpose of the present study. In order to do so, we have observed SH intensity images of an arsenic (As) ion implanted Si(111) substrate in a wide photon energy range from $2\hbar\omega=1.96$ to 5.19 eV, and have compared the SH intensity images with the linear optical reflection images. Although there have been several SHG experiments on ion implanted Si substrates,[22,23] no SH intensity images have been reported.

In Sec. II, preparation of the As-doped Si sample and the measurement conditions of the SH microscopy are described. In Sec. III, measured data of SH intensity images, linear optical reflection images, and Raman spectra of the Si sample are presented. Our measured SH intensity images show that contrast between the As-doped area and the nondoped area depends greatly on the SH photon energy. It is also found that the contrast in the SH intensity images is different from that in the linear optical reflection images. The origin of the contrast in the SH intensity images is also discussed in Sec. III. Sec. IV presents our conclusions and plans for future work.

[a]Author to whom correspondence should be addressed; electronic mail: h-sano@jaist.ac.jp

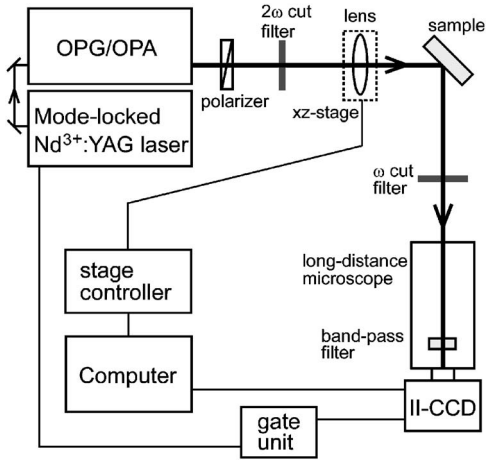

FIG. 1. Experimental setup for the second harmonic (SH) microscopy.

II. METHODOLOGY

The sample for the SH image observation was a high-dose As ion implanted *n*-type Si(111) wafer with a resistivity of $\rho=0.005-0.018\ \Omega$ cm before implantation. After forming a 580 nm thick oxide layer on the Si substrate, a part of the oxide layer was removed by photolithography, and the remaining oxide layer served as a mask pattern for the ion implantation. As ions were implanted into the Si wafer at an acceleration voltage of 40 kV with a dose of $\sim 10^{17}\ \mathrm{cm}^{-2}$, and the remaining oxide layer was removed by etching in a HF solution. No heat treatment of the sample was done after the ion implantation. Since the prepared sample was kept in air, a thin oxide layer was formed on the surface.

A high-dose ion implantation can lead to disordering of the crystal structure in the Si substrate. In order to evaluate this disordering, Raman spectra of the ion-implanted substrate near the bulk phonon band at $\sim 520\ \mathrm{cm}^{-1}$ were measured. The wavelength and the power of the incident beam were 488 and 4.5 mW, respectively. The energy resolution of the Raman spectrometer was $2\ \mathrm{cm}^{-1}$.

The setup of the SH microscope system used in the present study is shown in Fig. 1. The light source of the fundamental frequency was an optical parametric generator/amplifier (OPG/OPA) system (Ekspla PG401VIR/SH) driven by a frequency-tripled mode-locked Nd:YAG laser (Ekspla PL-2143B). The spectral bandwidth of the laser beam was narrower than 1 meV, the pulse duration time was 25 ps, and the repetition rate was 10 Hz. The plane of incidence was parallel to the $[1\bar{1}0]$ direction, and the incident angle was 45° from the surface normal. The incident beam was *p*-polarized, and its power was $55-450\ \mu\mathrm{J/pulse}$ at the sample surface. The reflected light from the sample was passed through a colored glass filter blocking the fundamental light, introduced into a long-distance microscope (Quester QM-1) with a bandpass filter, and detected by a time-gated image intensified charge coupled device (CCD) camera (Hamamatsu PMA-100). The spatial resolution of this microscope system was $\sim 3\ \mu$m. A typical accumulation time to obtain one SH intensity image was 450 min. The sensitivity of the detection system was calibrated by using the SH signal from the α-SiO_2 (0001) surface. Linear optical reflection images were obtained by replacing the OPG/OPA with a monochromated Xe lamp source in the SH microscopy system shown in Fig. 1. For measuring linear optical reflectivity spectra, a Si photodiode was used as a detector. All optical experiments were performed in air at room temperature.

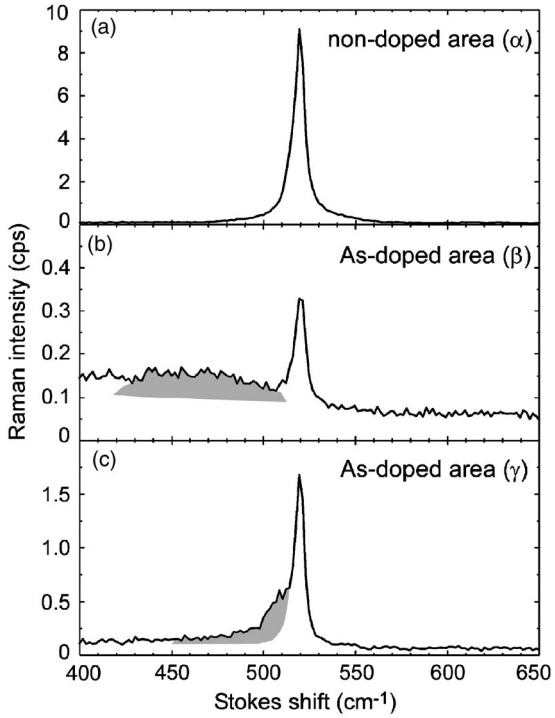

FIG. 2. Raman spectra of the Si phonon band of (a) nondoped and [(b) and (c)] As-doped areas. The areas α, β, and γ are defined in Fig. 3(i). The shadowed parts in the spectra of (b) and (c) represent the contribution of amorphous structure.

III. RESULTS AND DISCUSSION

To begin with, we discuss the crystal quality of the doped Si substrate. Figures 2(a)–2(c), are the Raman spectra of the nondoped area α, and the As-doped areas β and γ of the Si substrate, respectively. The areas α, β, and γ are defined in Fig. 3(i), and they exhibited different SH intensities as fully described below. As shown in Fig. 2, the intensity of the Raman peak at $\sim 520\ \mathrm{cm}^{-1}$ of the As-doped areas was much smaller than that of the nondoped area, and is accompanied by broad structures (shadowed parts)[24] on the lower energy side. According to Ref. 24, Figs. 2(b) and 2(c) are typical Raman spectra from Si with a disordered structure. Therefore, we can say that the As-doped area had an amorphous structure within the detection depth of the Raman measurement, i.e., ~ 50 nm.

Figures 3(a)–3(h) are the SH intensity images of the As-doped Si substrate for the SH photon energy from $2\hbar\omega = 1.96$ to 5.19 eV. The observed SH photons are represented by white dots. The contrast between the doped and nondoped areas is clearly seen in Figs. 3(a)–3(h). For $2\hbar\omega > 3$ eV the SH intensity from the nondoped area is larger than that from the doped area, but the contrast is reversed for $2\hbar\omega \leq 2.33$ eV. Figures 3(a)–3(c) also show that a part of the doped area (γ) emits stronger SH light. SH intensity in the area γ is not uniform, and bright structures with the size of a

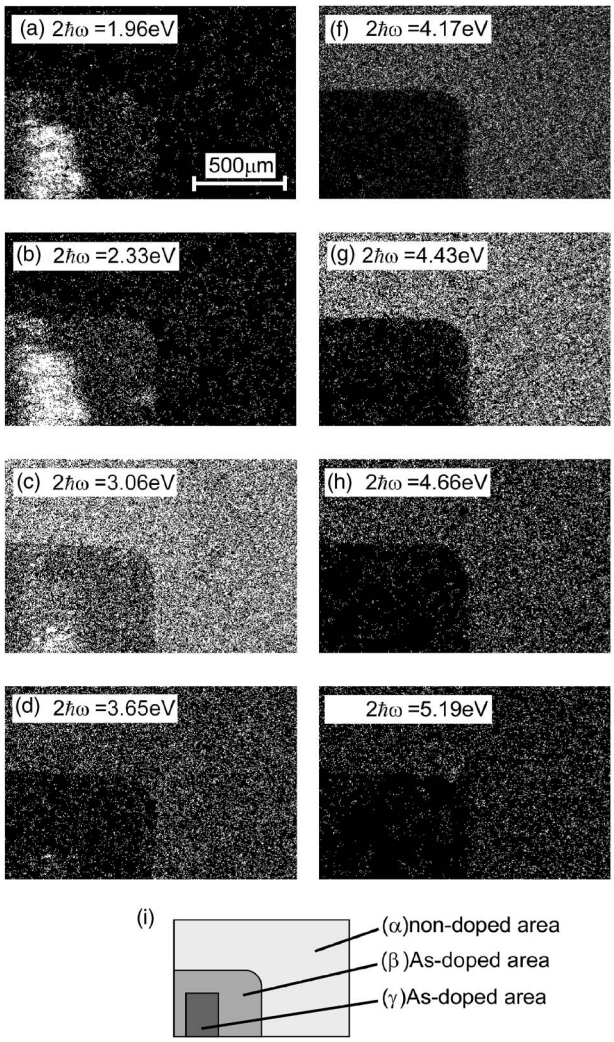

FIG. 3. SH intensity images of an As-doped Si substrate at the SH photon energy from $2\hbar\omega=1.96$ to 5.19 eV. The white dots represents the observed SH photons. The doped pattern is illustrated in (i).

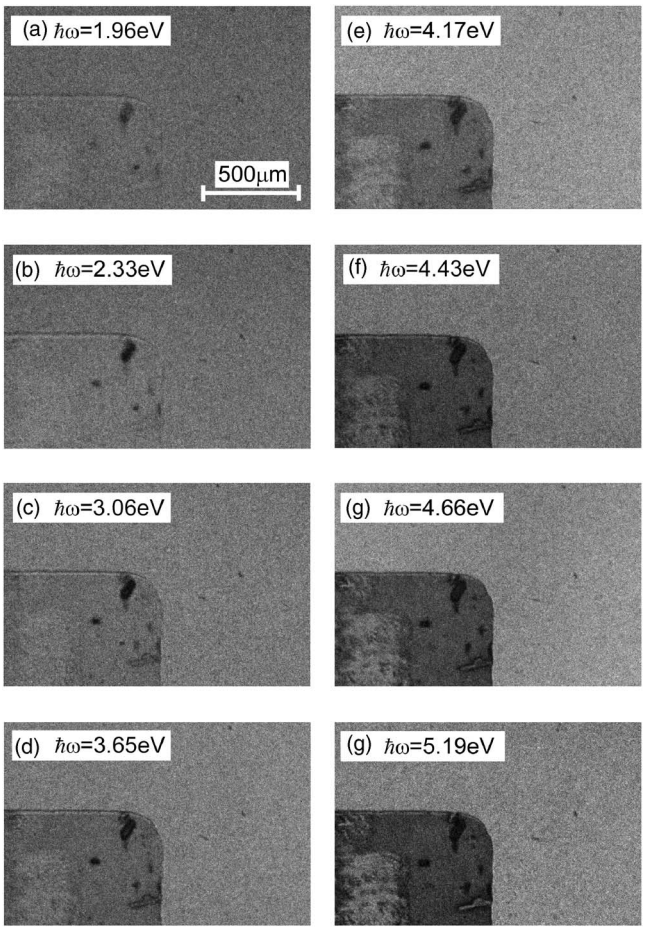

FIG. 4. Linear optical reflection images of an As-doped Si substrate at the incident photon energy from $\hbar\omega=1.96$ to 5.19 eV. The reflectivity is high where the image is bright.

few tens of micrometers are seen. The observed SH intensity images are expected to represent the spatial distribution of the electronic states of a Si substrate modified by the ion implantation. In order to confirm the validity of this expectation, it is necessary to clarify the origin of the measured SH signal.

Next, we discuss the origin of the contrast in the observed SH intensity images. The measured SH signal $I_{\mathrm{out}}(2\omega)$ is given by

$$I_{\mathrm{out}}(2\omega) = A\left|\chi^{(2)}\right|^2 I_{\mathrm{in}}^2(\omega). \tag{1}$$

Here, $I_{\mathrm{in}}(\omega)$ is the intensity of the incident light, A is a coefficient including Fresnel factors for incident and output fields, and $\chi^{(2)}$ is a second-order nonlinear susceptibility. Equation (1) indicates that the SH intensity depends not only on the nonlinear susceptibility but also on the linear optical property through the Fresnel factors. Hence, both the linear and nonlinear optical properties of the sample must be considered as candidate origins of the contrast in the SH intensity images.

As a beginning, we consider the linear optical property. Figure 4 shows linear reflection images of the As-doped Si substrate as a function of the photon energy. The observation photon energies in Figs. 4(a)–4(h) are the same as those in Figs. 3(a)–3(h). In Figs. 3 and 4, one can find an obvious difference between the SH and linear reflection images in the contrast among the α, β, and γ areas. For example, though the linear reflectivity of the doped area γ is larger than that of the doped area β in Fig. 4(f), no clear contrast between the doped areas β and γ can be seen in Fig. 3(f). If the SH intensity depends only on the linear optical property, the difference in the SH intensity between the doped areas β and γ should be observable. Therefore, it is likely that in the present case the nonlinear property considerably contributes to the contrast in the SH intensity. From a viewpoint of application of optical microscopy, this result is interesting because it demonstrates a spectroscopic microscopy capable of capturing information different from that obtained by conventional linear optical microscopy.

Figure 5 shows the SH intensity from the nondoped area α and the doped areas β and γ as a function of the SH photon energy $2\hbar\omega$. A peak is seen around $2\hbar\omega=4.4$ eV in the SH intensity from the nondoped area α (dashed line). This result agrees well with the SH spectra of Si(100) and Si(111) surfaces with thin oxide layers.[25–27] These previous studies reported that a strong resonant SHG enhancement arises from direct optical transitions of the bulk Si E_1

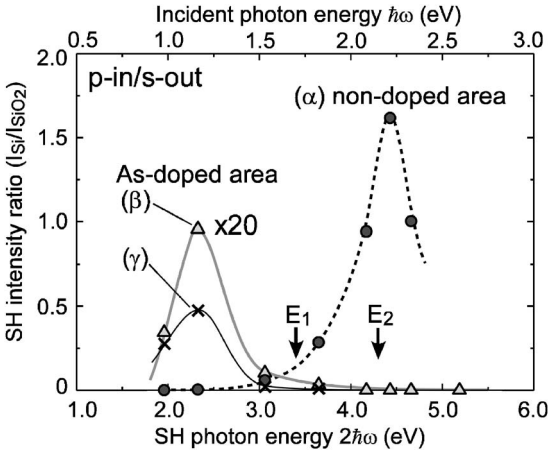

FIG. 5. SH intensity as a function of the SH photon energy for nondoped area α (circle) and As-doped areas β (triangle) and γ (cross). The areas α, β, and γ are defined in Fig. 3(i). The SH intensity of the As-doped area β (triangle) is magnified to 20 times the original intensity. Dashed line and gray and black solid lines are guides to the eyes.

(3.4 eV) and E_2 (4.3 eV) gaps in a few monolayers of strained Si at the $Si-SiO_2$ interface. The same mechanism probably occurs in the nondoped area of our Si(111) surface.

On the other hand, the SH intensity from the doped area is very small for $2\hbar\omega \gg 3.5$ eV, as shown in Figs. 3(d)–3(h) and 5. This result is consistent with those of the previous study[25] that an amorphous Si substrate exhibits no resonant SHG enhancement due to the E_1 and E_2 transitions. To discuss the origin of the very small SHG signal from the doped area, let us examine the linear optical reflectivity spectra in Fig. 6.[28] In Fig. 6, large reflectivity peaks corresponding to the E_1 and E_2 transitions are seen at 3.4 and 4.5 eV for the nondoped area (dashed line), while these peaks are not seen for the doped area (black and gray solid lines). This result distinctly indicates that the joint density of states (JDOS) of the E_1 and E_2 transitions for the doped area becomes small due to the disordering of the Si crystal structure. Therefore, the resonant effect of the E_1 and E_2 transitions on the SHG probably disappears and the SH intensity from the doped area becomes very small.

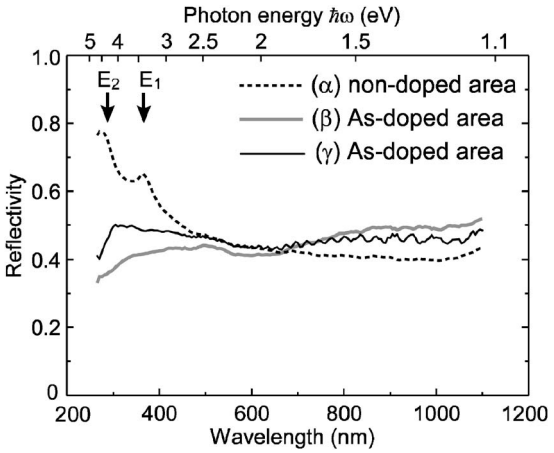

FIG. 6. Linear optical reflectivity as a function of the wavelength for nondoped area α (dashed line), As-doped areas β (gray solid line), and γ (black solid line). The areas α, β, and γ are defined in Fig. 3(i).

Next, we discuss the origin of the contrast in the SH intensity images for $2\hbar\omega \leqslant 2.33$ eV. In this energy range, the SH intensity from the nondoped area is smaller than that from the doped area, as can be seen in Fig. 5. The reason for the smaller SH intensity from the nondoped area is that the SH photon energy is far from the E_1 and E_2 resonances of the crystalline Si. On the other hand, the SH intensity from the doped area shows small resonant enhancement around $2\hbar\omega = 2.3$ eV, as shown in Fig. 5. At present, the origin of this resonant SH peak has not yet been clarified. However, we suggest the following two possible origins. The one is that the energy levels created by the As ion implantation led to the resonant SHG enhancement around $2\hbar\omega = 2.3$ eV. The other is that the disordering of the crystal structure slightly breaks the law of momentum conservation in the optical process,[29] so that the optical transition of the indirect band gap of the bulk Si crystal located at 1.1 eV becomes possible in the SHG.

Next, let us look closely at the doped area γ emitting strong SH light in Figs. 3(a) and 3(b). According to Ref. 24, the measured Raman spectra in Fig. 2 indicate that the disordering of crystal structure in the area γ is smaller than that in area β. However, we do not expect this difference in the crystal structure to be the origin of the SHG enhancement for the area γ because the SH intensity of the nondoped area, indicating no disordering of the crystal structure, is very small for $2\hbar\omega \leqslant 2.33$ eV.

Here, we suggest the following possible origin of the SHG enhancement for area γ. In Fig. 6, a periodic oscillation of reflectivity is seen in the range above 700 nm only for area γ (black solid line). This oscillation must result from the interference of the incident light. Namely, there must be a considerable discontinuity in the refractive index at a few micrometers below the surface so that the reflected light from the surface can interfere with the reflected light coming from this discontinuity. The discontinuity in the refractive index might have come from a thin air gap inside the Si substrate formed by exfoliation of a Si layer. Since the Si surface layer must be highly stressed by the high-dosed As atoms and the (111) face is a face of easy cleavage, the Si layer in the doped area γ may have possibly peeled off. In this case, the fundamental light for SHG is also reflected at the discontinuity, and this upward-propagating electric field can generate SH radiation very efficiently.[13] The SHG enhancement due to the same mechanism has been observed in the case of a GaAs slab structure.[13] At present, this mechanism is suggested to be the most likely origin of the SHG enhancement for the area γ.

In the present study, we have demonstrated that the spatial distribution of the electronic states of the As ion implanted Si(111) substrate can be observed with wavelength tunable optical SH microscopy. Since the As-doped area used in this study was relatively large, one may point out that spectroscopic data could be obtained with a focused fundamental beam only. However, let us see small bright structures with the size of a few tens of micrometers in the As-doped area γ of Figs. 3(a)–3(c). The resonant behavior of these structures would never been observed without the SH microscopy. The obtained results suggest that the spectroscopic

SH microscope will be a powerful tool for analyzing electronic states in small domains on semiconductor surfaces. As an example, the hydrogen deficiency of a hydrogen terminated Si surface by UV light irradiation will be an interesting study using the spectroscopic SH microscopy.[30] The UV light irradiation induces hydrogen desorption from the Si surface, forming some surface electronic levels due to the dangling bonds around the Fermi level. Since SHG has high surface sensitivity, these surface electronic states can be easily detected. This study will provide useful basic data for understanding the mechanisms of photoinduced desorption and photochemical vapor deposition (PCVD).

IV. CONCLUSION

The purpose of this study was to demonstrate that spectroscopic SH intensity images of a centrosymmetric crystal can be observed, and the SH microscopy provide different informations on electronic states from that associated with the linear optical response. This purpose was achieved by observing the SH intensity images of the As ion implanted Si(111) substrate in the photon energy range from $2\hbar\omega = 1.96$ to 5.19 eV. The results indicated that clear SH intensity images of the Si(111) substrate could be obtained, and that their contrast variance as a function of the SH photon energy was different from that of the linear optical reflection images. It is suggested that the origin of the contrast in the SH intensity images is mostly the resonant SHG enhancement effect arising from the optical electronic transitions between the electronic levels in the As-doped Si substrate. From the viewpoint of developing an original surface analysis method, the most important result in the present study is the fact that electronic resonant images of the Si surface were obtained with spectroscopic SH microscopy. At present, a full interpretation of the measured SH intensity images is rather difficult. Thus, an interpretation methodology based on the theoretical calculation of the SH signal[31] will be required for further development of spectroscopic SH microscopy.

[1]T. F. Heinz, in *Nonlinear Surface Electromagnetic Phenomena*, edited by H.-E. Ponath and G. I. Stegeman (North-Holland, Amsterdam, 1991), p. 353.
[2]G. Lüpke, Surf. Sci. Rep. **35**, 75 (1999).
[3]N. Bloembergen, Appl. Phys. B: Lasers Opt. **68**, 289 (1999).
[4]Th. Rasing, J. Magn. Magn. Mater. **175**, 35 (1997).
[5]S. Sioncke, T. Verbiest, and A. Persoons, Mater. Sci. Eng., R. **R42**, 115 (2003).
[6]M. Fiebig, D. Fröhlich, St. Leute, and R. V. Pisarev, Appl. Phys. B: Lasers Opt. **66**, 265 (1998).
[7]V. Kirilyuk, A. Kirilyuk, and Th. Rasing, Appl. Phys. Lett. **70**, 2306 (1997).
[8]S. Kurimura and Y. Uesu, J. Appl. Phys. **81**, 369 (1997).
[9]I. I. Smolyaninov, H. Y. Liang, C. H. Lee, and C. C. Davis, J. Appl. Phys. **89**, 206 (2001).
[10]S. I. Bozhevolnyi, J. M. Hvam, K. Pedersen, F. Laurell, H. Karlsson, T. Skettrup, and M. Belmonte, Appl. Phys. Lett. **73**, 1814 (1998).
[11]H. Tanaka, H. Kurokawa, E. Kobayashi, H. Sano, G. Mizutani, and S. Ushioda, Prog. Cryst. Growth Charact. Mater. **33**, 129 (1996).
[12]Y. Sonoda, G. Mizutani, H. Sano, S. Ushioda, T. Sekiya, and S. Kurita, Jpn. J. Appl. Phys., Part 2 **39**, L253 (2000).
[13]H. Sano, T. Shimizu, G. Mizutani, and S. Ushioda, J. Appl. Phys. **87**, 1614 (2000).
[14]C.-K. Sun, S.-W. Chu, S.-P. Tai, S. Keller, U. K. Mishra, and S. P. Denbaars, Appl. Phys. Lett. **77**, 2331 (2000).
[15]J. Erland, S. I. Bozhevolnyi, K. Pedersen, J. R. Jensen, and J. M. Hvarn, Appl. Phys. Lett. **77**, 806 (2000).
[16]P. J. Campagnola, M.-D. Wei, L. Lewis, and L. M. Loew, Biophys. J. **77**, 3341 (1999).
[17]P. J. Campagnola, A. C. Millard, M. Terasaki, P. E. Hoppe, C. J. Malone, and W. A. Mohler, Biophys. J. **82**, 493 (2002).
[18]P. Stoller, K. M. Reiser, P. M. Celliers, and A. M. Rubenchik, Biophys. J. **82**, 3330 (2002).
[19]G. Mizutani, Y. Sonoda, H. Sano, M. Sakamoto, T. Takahashi, and S. Ushioda, J. Lumin. **87–89**, 824 (2000).
[20]T. F. Heinz, F. J. Himpsel, E. Palange, and E. Burstein, Phys. Rev. Lett. **63**, 644 (1989).
[21]R. D. Schaller, J. C. Johnson, K. R. Wilson, L. F. Lee, L. H. Haber, and R. J. Saykally, J. Phys. Chem. B **106**, 5143 (2002).
[22]I. V. Kravetsky, L. L. Kulyuk, J. F. McGilp, M. Cavanagh, S. Chandola, J. Boness, G. Marowsky, and F. Harbsmeier, Surf. Sci. **402–404**, 542 (1998).
[23]K. Lo, Y. Wang, and J. Jin, Thin Solid Films **420–421**, 345 (2002).
[24]R. Alben, D. Weaire, J. E. Smith, Jr., and M. H. Brodsky, Phys. Rev. B **11**, 2271 (1975); T. Kamiya, M. Kishi, A. Ushirokawa, and T. Katoda, Appl. Phys. Lett. **38**, 377 (1981).
[25]G. Erley and W. Daum, Phys. Rev. B **58**, R1734 (1998).
[26]W. Daum, H.-J. Krause, U. Reichel, and H. Ibach, Phys. Rev. Lett. **71**, 1234 (1993).
[27]W. Daum, H.-J. Krause, U. Reichel, and H. Ibach, Phys. Scr., T **T49**, 513 (1993).
[28]Our measured reflectivity spectra of As-doped Si are consistent with dielectric functions reported by X.-F. He, R.-R. Jiang, R.-X. Chen, and D. Mo, J. Appl. Phys. **66**, 5261 (1989).
[29]D. Kovalev, H. Heckler, M. Ben-Chorin, G. Polisski, M. Schwartzkopff, and F. Koch, Phys. Rev. Lett. **81**, 2803 (1998).
[30]Y. Miyauchi, H. Sano, and G. Mizutani, e-J. Surf. Sci. Nanotechnol. **4**, 105 (2006).
[31]H. Sano and G. Mizutani, e-J. Surf. Sci. Nanotechnol. **1**, 57 (2003).